Notes on the Turing Instability and Chemical Instabilities

Michael Cross April 25, 2006

Introduction

In these notes, I discuss in more detail the nonlinear evolution equations and their linear stability analysis for chemicals that react and diffuse in solutions. Historically, such a linear stability analysis of a uniform state was first carried out in 1952 by Alan Turing [9]. He suggested the radical and highly stimulating idea that reaction and diffusion of chemicals in an initially uniform state could explain **morphogenesis**, how biological patterns arise during growth. Although reaction-diffusion systems are perhaps the easiest to study mathematically of the many experimental systems considered in this book, they have the drawback that quantitative comparisons with experiment remain difficult. The reason is that many chemical reactions involve short-lived intermediates in small concentrations that go undetected, so that the corresponding evolution equations are incomplete. Still, reaction diffusion systems are such a broad and important class of nonequilibrium systems—prevalent in biology, chemistry, ecology, and engineering—that a detailed discussion is worthwhile.

Turing Instability

Realistic equations describing chemical reactions in experimental geometries are complicated to formulate and difficult to investigate. The same was true in the 1940s when Alan Turing was thinking about morphogenesis. These difficulties did not stop Turing who, in the tradition of great theoretical science, set as his goal not the quantitative explanation of morphogenesis but the discovery of a clear plausible mechanism that could guide researchers in how to think about such a complex phenomenon. Indeed, the opening paragraph of his 1952 paper begins with these classic words[1]

> In this section a mathematical model of the growing embryo will be described. This model will be a simplification and an idealization, and consequently a falsification. It is to be hoped that the features retained for discussion are those of greatest importance in the present state of knowledge.

We will follow Turing in his 1952 paper and examine analytically the linear stability analysis of the simplest possible reaction-diffusion system that forms a pattern from a uniform state. The analysis will lead to several insights, some unexpected. One insight is that at least two interacting chemicals are needed for pattern formation to occur. Second is Turing's most surprising insight, that diffusion in a reacting chemical system can actually be a destabilizing influence. This is contrary to intuition since diffusion by itself smooths out spatial variations of a concentration field and so would be considered stabilizing. A third insight is that the instability caused by diffusion can cause the growth of structure at a particular wave length. This provides a possible mechanism for producing patterns like the segmentation patterns in the developing fly embryo, the periodic arrangement of tentacles around the mouth of the Hydra organism (a member of the Cnidaria

[1] The technical level of Turing's paper is about the level of the present discussion and I encourage you to read this visionary paper. The paper has many bold and interesting ideas that draw upon Turing's interdisciplinary thinking about biology, chemistry, and mathematics. His paper is also interesting from a historical point of view, to see what facts Turing used to develop his hypotheses. For example, Turing could only speculate about how an organism knew how to grow since the role of DNA would only be announced a year later in 1953. The last section of the paper mentions one of the first simulations on a digital computer and Turing states his belief that these new computers will be important for future research. There is a certain irony here since Turing was one of the inventors of the digital computer.

phylum), or zebra stripes. A fourth insight (which was not clearly stated until after Turing's paper) is that pattern formation in a chemical system will not occur unless the diffusion coefficients of at least two reagents differ substantially. The difficulty of satisfying this condition for chemicals in solution partially explains why nearly 40 years passed after Turing's paper before experiments were able to demonstrate the truth of his ideas.

Reaction-Diffusion Equations

We will study the **Turing model** [2] for two reacting and diffusion chemicals of the form:

$$\partial_t u_1 = f_1(u_1, u_2) + D_1 \partial_x^2 u_1, \tag{1a}$$

$$\partial_t u_2 = f_2(u_1, u_2) + D_2 \partial_x^2 u_2, \tag{1b}$$

or in vector form

$$\partial_t \mathbf{u} = \mathbf{f}(\mathbf{u}) + \mathbf{D}\partial_x^2 \mathbf{u}, \tag{2}$$

where we have introduced a diagonal 2×2 **diffusion matrix D** defined by

$$\mathbf{D} = \begin{pmatrix} D_1 & 0 \\ 0 & D_2 \end{pmatrix}. \tag{3}$$

Eq. (1) describes the evolution of two concentration fields $u_i(t, x)$ on the real line $-\infty < x < \infty$. The nonlinear functions $f_i(u_1, u_2)$ are the reaction rates of the two chemicals while the D_i are the corresponding diffusion coefficients. The simplest possible model is obtained by assuming that there is no prior spatiotemporal structure in the system so that the functions f_i and the diffusion coefficients D_i do not depend explicitly on time t or on position x. For simplicity, we further assume that the diffusion coefficients are constants and so do not depend on the field values u_i. These assumptions are all quite reasonable for many experimental situations.

Equations (1) cannot accurately describe a sustained nonequilibrium chemical system since they incorporate no way to feed reactants into and remove products from the system. The neglect of a transverse confined coordinate along which such feed might occur is a major simplification. An accurate treatment of the feed direction introduces complicated spatial structure. Actually many early experiments on pattern formation in chemical reactions could be rather well approximated by ignoring the confined coordinate. Typically these experiments were done using a thin layer of chemicals in a petri dish, or chemicals soaked in filter paper. The variation of chemical concentration across the layer or thickness of filter paper is perhaps small in these experiments (typically the conditions are not well controlled, so this is just an assumption). A reduction to equations describing just the spatial variation in the plane (ie. Eqs. (1) but with $\partial_x^2 \to \nabla^2 = \partial_x^2 + \partial_y^2$) would be a reasonable approximation. However, in these experiments, since there is no feed of refreshed chemicals to sustain the reactions, any pattern formation or dynamics is a *transient*, and eventually the system would approach a uniform chemical equilibrium. This difficulty may be hidden in the simple reduced equations (1) by approximating some dynamical chemical concentrations as constants in the reaction term $\mathbf{f}(\mathbf{u})$.

Linear Stability Analysis

We now perform the linear stability analysis of uniform solutions of the two-chemical reaction-diffusion model Eq. (1). Turing's surprising and important discovery was that there are conditions under which

[2] In his paper, Turing examined two kinds of models, spatially coupled odes that modelled discrete biological cells and coupled pdes of the form that we analyze here, that treated the tissue as a continuous medium.

the spatially uniform state is *stable* in the absence of diffusion[3] but can become *unstable* to nonuniform perturbations precisely because of diffusion. Further, for many conditions the instability first occurs at a finite wave length and so a cellular pattern starts to appear.

For simplicity, we will discuss the one-dimensional case. If we assume that the evolution equations have rotational symmetry in higher dimensions, the two- and three-dimensional cases are identical *mutatis mutandis*: the one-dimensional Laplacian ∂_x^2 becomes a higher-dimensional Laplacian ∇^2, the combination qx becomes everywhere a dot product $\mathbf{q} \cdot \mathbf{x}$ with a wave vector $\mathbf{q}$, and the wave number square q^2 becomes the quantity $\mathbf{q} \cdot \mathbf{q}$.

The following discussion is not mathematically difficult but has many details. You will likely best appreciate the discussion if you take your time and derive the results for yourself in parallel with the text. The goal of the discussion is to derive, and then to understand physically, conditions that are sufficient for the real parts of all growth rates to be negative. When these conditions are first violated and instability occurs, it is then important to think about the values of the wave numbers corresponding to the fastest growing modes.

We begin by assuming that we have somehow found a stationary uniform base solution $\mathbf{u}_b = (u_{1b}, u_{2b})$. This satisfies the Turing model with all partial derivatives set to zero, leading to $\mathbf{f}(\mathbf{u}_b) = \mathbf{0}$ or

$$f_1(u_{1b}, u_{2b}) = 0, \tag{4a}$$

$$f_2(u_{1b}, u_{2b}) = 0. \tag{4b}$$

These are two nonlinear equations in two unknowns. Finding a uniform solution can be hard since there is no systematic way to find even a single solution of a set of nonlinear equations. Numerical methods such as the Newton method can find accurate approximations to solutions of nonlinear equations but only if a good guess for a solution is already known. For two nonlinear equations like Eq. (4), a graphical way to find solutions that is sometimes useful is to plot the **nullclines** of each equation. An equation of the form $f_1(u_1, u_2) = 0$ defines an implicit relation $u_2 = g_1(u_1)$ between the two variables u_1 and u_2 called the nullcline of that equation. If the functions $f_i(u_1, u_2)$ are sufficiently simple, their nullclines $g_i(u_1)$ can sometimes be found explicitly and then plotted on a single plot with axes labelled by u_1 and u_2. Any intersection of the two nullclines is then a solution of the nonlinear equations.

By linearizing about the base state $\mathbf{u}_b$, you can show that an arbitrary infinitesimal perturbation $\delta\mathbf{u}(t, x) = (\delta u_1(t, x), \delta u_2(t, x))$ of the base state will evolve in time according to the following linear constant-coefficient evolution equations:

$$\partial_t \delta u_1 = a_{11}\delta u_1 + a_{12}\delta u_2 + D_1 \partial_x^2 \delta u_1, \tag{5a}$$

$$\partial_t \delta u_2 = a_{21}\delta u_1 + a_{22}\delta u_2 + D_2 \partial_x^2 \delta u_2. \tag{5b}$$

The constant coefficients a_{ij} come from the 2×2 Jacobian matrix $\mathbf{A} = \partial\mathbf{f}/\partial\mathbf{u}$ evaluated at the constant base solution $\mathbf{u}_b$,

$$a_{ij} = \left.\frac{\partial f_i}{\partial u_j}\right|_{\mathbf{u}_b}. \tag{6}$$

The mathematical structure of Eqs. (5) can be clarified by writing them in vector form:

$$\partial_t \delta\mathbf{u} = \mathbf{A}\delta\mathbf{u} + \mathbf{D}\partial_x^2 \delta\mathbf{u}, \tag{7}$$

where $\mathbf{D}$ is the 2×2 diffusion matrix previously introduced in Eq. (3). Because Eq. (7) is linear with constant coefficients and because the boundaries are periodic or at infinity, we can use translational symmetry to seek

[3] Diffusion can be suppressed in several ways. Mathematically, we simply set the diffusion coefficients to zero. Experimentally, we can stir the chemicals to eliminate spatial nonuniformity.

a particular solution $\delta\mathbf{u}(t,x)$ that is a constant vector $\delta\mathbf{u}_q$ times an exponential in time times an exponential in space:

$$\delta\mathbf{u} = \delta\mathbf{u}_q\, e^{\sigma_q t}\, e^{iqx} = \begin{pmatrix} \delta u_{1q} \\ \delta u_{2q} \end{pmatrix} e^{\sigma_q t} e^{iqx}, \tag{8}$$

with growth rate σ_q and wave number q. *Note that both components of the perturbation vector* $\delta\mathbf{u}$ *have the* ***same*** *dependence on time and space.* Only with this assumption can the spatial and temporal dependencies be eliminated completely from the linearized evolution equations and a simple solution found.

If we substitute Eq. (8) into Eq. (7), divide out the exponentials, and collect some terms, we obtain the following eigenvalue problem

$$\mathbf{A}_q\, \delta\mathbf{u}_q = \sigma_q\, \delta\mathbf{u}_q, \tag{9}$$

where the the 2×2 real matrix $\mathbf{A}_q$ is defined by

$$\mathbf{A}_q = \mathbf{A} - \mathbf{D}q^2 = \begin{pmatrix} a_{11} - D_1 q^2 & a_{12} \\ a_{21} & a_{22} - D_2 q^2 \end{pmatrix}. \tag{10}$$

Eq. (9) tells us that the growth rate σ_q and constant vector $\delta\mathbf{u}_q$ form an eigenvalue-eigenvector pair of the matrix $\mathbf{A}_q$, and that there is one such 2×2 eigenvalue problem for each wave number q. The eigenvalue problem for a given q has generally two linearly independent eigenvectors that we will denote by $\delta\mathbf{u}_{iq}$ for $i = 1, 2$. If the corresponding eigenvalues are σ_{iq}, the particular solution with wave number q will have the form:

$$\left(c_{1q}\, \delta\mathbf{u}_{1q}\, e^{\sigma_{1q}t} + c_{2q}\, \delta\mathbf{u}_{2q}\, e^{\sigma_{2q}t}\right) e^{iqx}, \tag{11}$$

where the coefficients c_{iq} are complex constants, that depend on the initial perturbation at $t = 0$[4]. This solution decays if $\mathrm{Re}(\sigma_{iq}) < 0$ for $i = 1, 2$. An arbitrary perturbation $\delta\mathbf{u}(t,x)$ is a superposition of expressions like Eq. (11) over all wave numbers q. The uniform solution $\mathbf{u}_b$ is stable if both eigenvalues σ_{iq} have negative real parts for all wave numbers q, i.e., if $\max_i \max_q \mathrm{Re}(\sigma_{iq}) < 0$.

The characteristic polynomial for the eigenvalue problem Eqs. (9,10) can be written

$$0 = \det\left(\mathbf{A}_q - \sigma_q \mathbf{I}\right) = \sigma_q^2 - (\mathrm{tr}\mathbf{A}_q)\sigma_q + \det \mathbf{A}_q \tag{12}$$

where $\mathrm{tr}(\mathbf{A}_q)$ denotes the trace (sum of diagonal elements) of the matrix $\mathbf{A}_q$ and $\det(\mathbf{A}_q)$ the determinant. The eigenvalues are then σ_{1q} and σ_{2q} given by

$$\sigma_q = \frac{1}{2}\mathrm{tr}\mathbf{A}_q \pm \frac{1}{2}\sqrt{(\mathrm{tr}\mathbf{A}_q)^2 - 4\det \mathbf{A}_q} \tag{13}$$

The regions of stability (both $\mathrm{Re}\,\sigma_q$ negative) and instability (at least one $\mathrm{Re}\,\sigma_q$ positive) in the $\mathrm{tr}\,A_q$ - $\det\, A_q$ plane are shown in Fig. 1. From this figure or the expression Eq. (13) a simple criterion can be derived that determines when the real parts of both eigenvalues are negative: *the trace of the matrix must be negative and the determinant of the matrix must be positive.* For the matrix $\mathbf{A}_q$ Eq. (10), these criteria for stability take the explicit form:

$$\mathrm{tr}\mathbf{A}_q = a_{11} + a_{22} - (D_1 + D_2)q^2 < 0, \tag{14a}$$

$$\det \mathbf{A}_q = (a_{11} - D_1 q^2)(a_{22} - D_2 q^2) - a_{12}a_{21} > 0. \tag{14b}$$

If both conditions hold for all wave numbers q, the stationary uniform base state $\mathbf{u}_b$ is linearly stable.

If Eq. (2) instead involved N interacting chemicals, we would need to solve a $N \times N$ eigenvalue problem Eq. (9) for each wave number q. For $N \geq 3$, analytical criteria that all the eigenvalues of a $N \times N$ matrix $\mathbf{A}_q$

[4] A real solution can be obtained as usual by adding the complex conjugate solution.

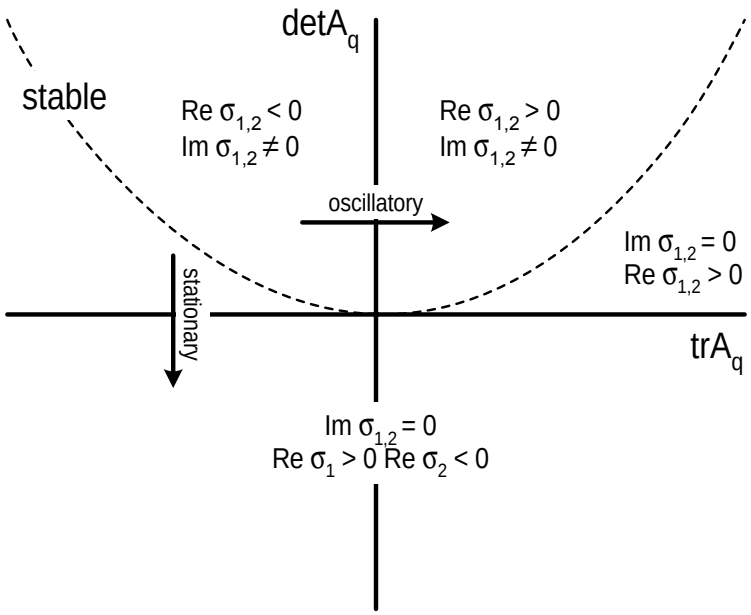

Figure 1: Stability regions of the Turing system in the trA$_q$ - det A$_q$ plane. The plot shows regions of different characteristics of the two eigenvalues σ_1 and σ_2 calculated from Eq. (12). The parabola $\det \mathrm{A}_q = \frac{1}{4}\mathrm{trA}_q$ divides the plane into two halves: above this curve the two eigenvalues are complex (and are complex conjugates of one another), below this curve both eigenvalues are real. The shaded region is the stable region, $\mathrm{Re}\,\sigma_{1,2} < 0$. Over the unshaded portion there is at least one eigenvalue with positive real part. A stationary instability occurs passing through the negative $\mathrm{tr}\,A_q$ axis to negative values of $\det A_q$, whereas an oscillator instability occurs passing through the positive $\det A_q$ axis to positive values of $\mathrm{tr}\,A_a$.

have negative real parts become cumbersome to derive and to work with[5] and so the case $N = 2$ that Turing discussed in his paper hits the mathematical sweet spot of being manageable and leading to interesting results. For experiments with $N > 3$ reacting chemicals, it is usually easiest to study the corresponding model by numerical methods. With modern computers and modern numerical algorithms, it is straightforward to find all the eigenvalues of a $N \times N$ matrix quickly for N as large as 10,000. As you can imagine, it would be exceedingly difficult to map out the reaction rates for so many interacting chemicals. Progress in studying the linear stability of chemical systems with large N is therefore limited by scientific knowledge, not by the ability to calculate eigenvalues.

We now discuss the physical meaning and implications of the mathematical criterion Eq. (14) in the context of pattern formation[6]. There are many abstract symbols and equations here and some careful thinking is needed to see how to extract some physical insights. A first step is to identify the precise scientific question of interest, not just the technical mathematical question of when some base state $\mathbf{u}_b$ becomes linearly unstable. Turing's insight was that diffusion of chemicals may somehow cause a pattern-forming instability. If so, then the starting point scientifically is to imagine that somehow the diffusion has been turned off (mathematically by setting the diffusion coefficients or the wave number q to zero, experimentally by stirring the solutions at high speed) and then we slowly turn on the diffusion to see if instability ensues. If we adopt this as our strategy, *then we need to assume that the reacting chemicals form a stable stationary state in the absence of*

[5]The book by Murray [4] has an appendix that discusses some necessary and sufficient analytical criteria that all the eigenvalues of a real $N \times N$ matrix have negative real parts. The **Routh-Hurwitz criterion** states that a certain sequence of determinants from size 1 to N all have to be positive. Determinants are difficult to work with symbolically since they involve a sum of $N!$ products of matrix elements.

[6]Our discussion here follows that of a paper by Segel and Jackson [6] that clarified Turing's original analysis.

diffusion. Setting the diffusion constants D_i to zero in Eq. (14), we obtain the following *criterion for linear stability of the uniform state in the absence of diffusion*:

$$a_{11} + a_{22} < 0, \tag{15a}$$

$$a_{11}a_{22} - a_{12}a_{21} > 0. \tag{15b}$$

If this criterion is satisfied, a well-mixed two-chemical solution will remain stable and uniform. Comparing Eq. (15a) with Eq. (14a) and remembering that diffusion constants D_i and the quantity q^2 are non-negative, we conclude that

$$\mathrm{tr}\mathbf{A}_q = a_{11} + a_{22} - (D_1 + D_2)q^2 < a_{11} + a_{22} < 0, \tag{16}$$

so the trace of the matrix $\mathbf{A}_q$ is always negative. We conclude that the only way for diffusion to destabilize the uniform state is for the second criterion Eq. (14b) to become reversed so that the determinant of $\mathbf{A}_q$ becomes negative.

The next step is therefore to figure out when the determinant $\det \mathbf{A}_q$ changes sign from positive to negative. Eq. (14b) tells us that the determinant $\det \mathbf{A}_q$ is a parabola in the quantity q^2 that opens upwards, being positive for $q^2 = 0$ by Eq. (15b) and positive for large q^2. A condition for linear instability in the presence of diffusion is then obtained by asking when the minimum value of this parabola first becomes negative. Setting the derivative of $\det \mathbf{A}_q$ with respect to q^2 to zero, we learn that the minimum occurs at the wave number q_m given by:

$$q_m^2 = \frac{D_1 a_{22} + D_2 a_{11}}{2D_1 D_2}. \tag{17}$$

The corresponding value of $\det \mathbf{A}_q$ at this minimum is

$$\det \mathbf{A}_{q_m} = a_{11}a_{22} - a_{12}a_{21} - \frac{(D_1 a_{22} + D_2 a_{11})^2}{4D_1 D_2}. \tag{18}$$

This expression is negative when the inequality

$$D_1 a_{22} + D_2 a_{11} > 2\sqrt{D_1 D_2 (a_{11}a_{22} - a_{12}a_{21})}, \tag{19}$$

is satisfied. The term inside the square root is positive because of Eq. (15b). As a corollary, Eq. (19) implies that

$$D_1 a_{22} + D_2 a_{11} > 0, \tag{20}$$

which can also be deduced directly from Eq. (17) since q_m^2 is a non-negative real number. From Eqs. (15a) and (20), we see that one of the quantities a_{11} and a_{22} must be positive and the other negative. For concreteness, let us choose $a_{11} > 0$ and $a_{22} < 0$ in the subsequent discussion. Then Eq. (15b) further implies that the quantities a_{12} and a_{21} must also have opposite signs.

Eq. (19) is a necessary and sufficient condition for linear instability of a uniform state that is stable in the absence of diffusion Eq. (15). As some experimental knob is turned, the matrix elements a_{ij} will change their values smoothly through their dependence on the experimental parameter. (Again, diffusion constants D_i can be considered constant for many experiments and so usually do not play the role of an easily varied bifurcation parameter.) At some parameter value, the inequality Eq. (19) may become true and the uniform state will become unstable to perturbations growing with a wave number close to the value q_m in Eq. (17).

The condition Eq. (19) can be expressed alternatively in terms of two **diffusion lengths**

$$l_1 = \sqrt{\frac{D_1}{a_{11}}} \qquad \text{and} \qquad l_2 = \sqrt{\frac{D_2}{-a_{22}}}, \tag{21}$$

in the form

$$q_m^2 = \frac{1}{2}\left(\frac{1}{l_1^2} - \frac{1}{l_2^2}\right) > \sqrt{\frac{a_{11}a_{22} - a_{12}a_{21}}{D_1 D_2}}. \tag{22}$$

This implies that the length l_2 must be sufficiently larger than the length l_1. Now our assumption that $a_{11} > 0$ implies that chemical 1 enhances its own instability and so could be called an *activator*. Similarly, since $a_{22} < 0$, chemical 2 inhibits its own growth and could be called an *inhibitor*. The necessary condition $l_2 > l_1$ for a Turing instability is then sometimes referred to as "local activation with long range inhibition."

The condition $l_2 > l_1$, when expressed in the equivalent form $D_2/D_1 > (-a_{22}/a_{11})$ partly explains why experimentalists had such a hard time finding a laboratory example of a Turing instability. The diffusion coefficient D_2 of the inhibitor has to exceed the diffusion coefficient D_1 of the inhibitor by a factor $(-a_{22})/a_{11}$ which can exceed 10 for some realistic models of reaction-diffusion experiments. Since the diffusion coefficients of most small ions in water have the same value of about $10^{-9}\,\mathrm{m}^2/\mathrm{sec}$, some ingenuity is required to create a Turing instability. Experimentalists found (by accident!) that one way to achieve a large disparity in diffusion coefficients was to introduce a third molecule (such as starch in the CDIMA reaction) that was fixed to an immobile matrix in the solution (the walls of the porous gel). The effective diffusion coefficient for a chemical that reversibly binds to this immobile molecule is substantially smaller than that for chemicals that do not bind.

The criteria Eq. (15) and Eq. (19) for the instability of a uniform state are rather abstract and so we now apply these criteria to a simple two-variable mathematical model known as the **Brusselator**[7] to illustrate the ideas. The Brusselator is a reaction-diffusion model that describes the evolution of two chemical concentrations $u_1(t, x)$ and $u_2(t, x)$:

$$\partial_t u_1 = a - (b+1)u_1 + u_1^2 u_2 + D_1 \partial_x^2 u_1, \tag{23a}$$

$$\partial_t u_2 = b u_1 - u_1^2 u_2 + D_2 \partial_x^2 u_2. \tag{23b}$$

The parameters a, b, D_1, and D_2 are positive constants. Although invented with the goal of understanding the Belousov-Zhabotinsky reaction and although successful in producing uniform oscillations and travelling waves, this model was intended not to describe a specific chemical experiment but to show how an invented plausible sequence of chemical reactions could reproduce qualitative but difficult to understand features of actual experiments. The context in which this model was invented suggests assigning the following parameter values

$$a = 1.5, \qquad D_1 = 2.8, \qquad D_2 = 22.4, \tag{24}$$

and varying the parameter b as the bifurcation parameter. We now show how to predict analytically for what value of b a uniform base state becomes linearly unstable.

A stationary uniform base state $\mathbf{u}_b = (u_{1b}, u_{2b})$ can be found by looking for solutions of Eq. (23) with all partial derivatives set to zero. It is straightforward to show that there is only one uniform state given by

$$u_{1b} = a, \qquad u_{2b} = \frac{b}{a}. \tag{25}$$

Please keep in mind that it is rarely this easy to find the stationary uniform state of some set of nonlinear evolution equations!

By linearizing the Brusselator model around this base state, you can show that the Jacobian matrix $\mathbf{A} = \partial \mathbf{f}/\partial \mathbf{u}$ is given by:

$$\mathbf{A} = \begin{pmatrix} a_{11} & a_{12} \\ a_{21} & a_{22} \end{pmatrix} = \begin{pmatrix} b-1 & a^2 \\ -b & -a^2 \end{pmatrix}. \tag{26}$$

[7] Two of the more widely studied models of reaction-diffusion dynamics are named after the geographical location where the model was invented. Thus the Brusselator is named after Brussels, Belgium, and the **Oregonator** is named after the state of Oregon in the United States.

The off-diagonal elements have opposite signs as required for a Turing instability, but the diagonal elements have opposite signs only if

$$b > 1. \tag{27}$$

When this inequality holds, we conclude that chemical 1 is an activator ($a_{11} > 0$) and that chemical 2 is an inhibitor ($a_{22} < 0$).

The uniform state is stable in the absence of diffusion when Eq. (15) holds, i.e.

$$\mathrm{tr}\mathbf{A} < 0 \quad \Longrightarrow \quad b < 1 + a^2 = 3.25, \tag{28a}$$

$$\det \mathbf{A} > 0 \quad \Longrightarrow \quad a^2 > 0. \tag{28b}$$

Only the first condition leads to a constraint, that the parameter b must be smaller than 3.25. Using the matrix elements Eq. (26) and the fact that $a_{11}a_{22} - a_{12}a_{21} = a^2$, the Segel-Jackson criterion for linear instability Eq. (19) can be manipulated into the form

$$b \geq \left(1 + a\sqrt{\frac{D_1}{D_2}}\right)^2. \tag{29}$$

The critical value b_c is determined by equality and the parameter values Eq. (24) imply

$$b_\mathrm{c} \approx 2.34. \tag{30}$$

The corresponding wave number q_c at instability is given by Eq. (17)

$$q_\mathrm{c} = \sqrt{\frac{D_1 a_{22} + D_2 a_{11}}{2D_1 D_2}} \approx 0.435, \tag{31}$$

which corresponds to a wave length of $2\pi/q_\mathrm{c} \approx 14.5$.

The onset of instability can be understood visually by plotting the maximum growth rate curve $\max_i \mathrm{Re}\sigma_{iq}$ as a function of the wave number q for values of the parameter b below, equal to, and above the critical value b_c (see Fig. 2). The maximum growth rate can be calculated explicitly as the maximum of the real part of the two eigenvalues σ_{iq} associated with each wave number q (recall the discussion associated with Eq. (11)). We summarize the results in Fig. 2. The growth rate σ_q is actually complex for small q (the dotted line in the figure indicates the imaginary part of the eigenvalue with the largest real part) but becomes real for larger q. In particular, the imaginary part is zero near the peak corresponding to the fastest growing mode. For a given parameter b, note how the curve $\max_i \mathrm{Re}(\sigma_{iq})$ has a kink —the slope changes discontinuously—because the eigenvalues switch from complex to real at this point.

Since the Brusselator does not describe an actual experiment, you may wonder whether it is possible to test independently the above predictions of the critical parameter b_c and critical wave number q_c. It is straightforward to write a computer code that integrates the evolution equations Eq. (23) in a large periodic interval. The parameter values could then be set to those of Eq. (24) and the initial conditions of the fields u_1 and u_2 set to be the uniform values Eq. (25) plus some random noise of tiny amplitude. For $b < b_\mathrm{c}$, the small-amplitude noise should decay exponentially and the fields will converge towards their uniform values. For b just larger than b_c, the uniform state should be unstable and a cellular structure with wave number close to Eq. (31) should appear. What happens in the long term as the exponential growth starts to saturate is not predicted by the linear stability analysis but would be revealed by the numerical integration. The unstable uniform state could evolve onto a stationary, periodic, quasiperiodic, or chaotic attractor.

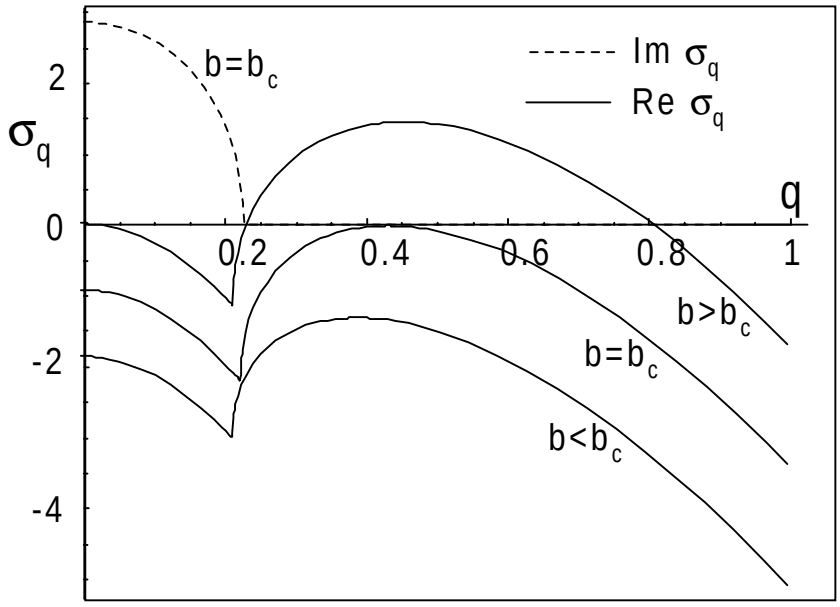

Figure 2: Solid curves: plots of the maximum real part of the growth rate, $\max_i \mathrm{Re}(\sigma_{iq})$ versus wave number q, for infinitesimal perturbations of the uniform state Eq. (25) of the Brusselator model Eq. (23), for the choice of parameters Eq. (24). Three curves are plotted corresponding to a b-parameter below instability ($b = 0.6b_c \approx 1.40$), to the critical value ($b = b_c \approx 2.34$), and above instability ($b = 1.4b_c \approx 3.28$). The critical wave number $q_c \approx 0.435$ is identified as the wave number for which the maximum real part of the growth rate first becomes zero. The wave number corresponding to the fastest growing mode increases slowly with increasing b. The dotted line is the imaginary part of the eigenvalue that has the maximum real part for $b = b_c$. The imaginary part for the other b values are not shown since they are nearly identical.

Oscillatory Instability

The focus of the analysis of the previous section was on the Turing instability: an instability first occurring at $q \neq 0$. However the analysis also shows that the two reaction diffusion equations may also show an oscillatory instability occurring at $q = 0$. This occurs when $\mathrm{tr}\, A_{q=0}$ passes to a positive value whilst $\det A_q$ is positive for all q. Since on the unstable side of a type III-o transition there is a band of growing oscillatory modes with wave numbers centered around zero, we might expect this system to support both spatially uniform nonlinear oscillations, and long wavelength nonlinear wave states.

In fact, at the same time Turing was doing his theoretical work on reaction-diffusion systems in Britain, a chemist in the Soviet Union, B. P. Belousov was observing oscillating chemical reactions in the laboratory. This work was not believed, since it was thought inconsistent with the idea that mixed chemicals must relax to equilibrium, and was rejected for publication.

Later Zhabotinsky continued the investigation and published work on both spatially uniform oscillations and wave states from the late 1960s onwards. It is now a common demonstration experiment to mix chemicals in a shaken test tube or stirred beaker, and watch the color periodically change (from blue to red and back for a modern version of the reaction used by Belousov). The shaking or stirring effectively mixes the chemicals, eliminating spatial inhomogeneities so that only spatially uniform ($q = 0$) oscillation is seen. In an unstirred petrie dish on the other hand, beautiful patters of propagating waves are seen. In most cases, experimental

chemical systems showing oscillations or waves are not near a linear instability, and the oscillations or waves are highly nonlinear, so that a description based on the linear modes is not quantitatively useful.

Realistic Chemical Systems

We now turn to realistic systems of reacting and diffusing chemicals that experimentalists use to study pattern formation in chemical systems. As is often the case, the apparatus is quite complex to approach the ideal conditions for which the phenomena is most cleanly seen, and might be quantitatively compared with theory. An additional difficulty in observing the Turing instability is that the diffusion constants of the some of the chemical participants must usually differ by a large ratio, which is hard to arrange for chemical reactions between small molecules in solution. This criterion does not apply for the study of oscillations and waves. The dynamical equations describing the evolution of the chemicals are also much more complicated than the simple two variable Turing system, and we spend some time explaining how the equations are deduced.

Experimental Apparatus

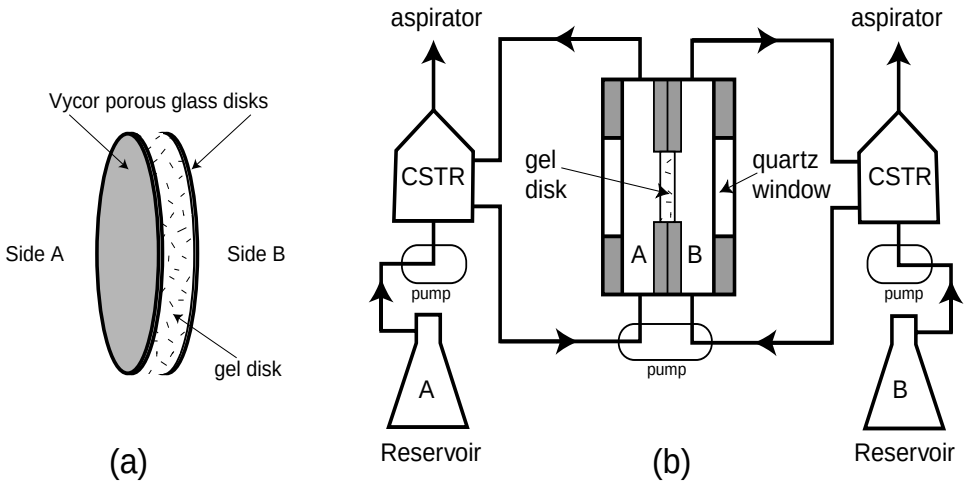

Figure 3: Schematic design of an experiment to study the pattern formation of reacting and diffusing chemicals in solution. (a) The chemical reactions take place near the middle of a uniform transparent porous gel 2 mm thick, that is confined between two wide (25 mm), thin (0.4 mm), uniform, porous, and transparent glass plates A and B. (b) Details of how the chemicals from two reservoirs are fed to the gel. Reservoirs A and B contain mixtures of chemicals that are inert by themselves but react when combined. The contents of these reservoirs are pumped into a "continuously fed stirred tank reactor" or CSTR where the solutions are mixed thoroughly so that the concentrations are spatially uniform. The contents of each CSTR are then pumped to provide a steady flow at known concentrations past the outer sides of the porous plates of Part (a). The chemicals diffuse through the porous plate into the gel, react, and reaction products diffuse out and are swept away. Pattern formation within the gel is visualized through a transparent quartz window. The gel is kept at a constant temperature throughout any given experiment. The chemical concentrations in the reservoirs or the temperature can be used as bifurcation parameters. [From the paper "Transition to Chemical Turbulence," Q. Ouyang and H. L. Swinney: Chaos **1,** 411 (1991)]

Fig. 3 shows schematically the design of a recent experiment that studied pattern formation of reacting and diffusing chemical solutions [5]. The flat parallel circular plates are made of a transparent porous glass

through which chemicals can diffuse and that allows visual observation of the pattern between the plates. The thin cylindrical volume between the plates is filled with a transparent uniform porous gel whose pores are so small (about 80 Å) that they suppress fluid motion. This simplifies the experiment conceptually since the pattern formation is due only to chemicals reacting and diffusing. The gel also renders the pattern visible by changing color according to the concentration of one of the reaction products. A system of reservoirs, pumps, and *continuously fed stirred tank reactors* (CSTRs) provides a constant flow of fresh reagents across the outer surfaces of plates A and B. As a result, these outer boundaries are surfaces of constant chemical concentrations for each of the reagents. The chemicals diffuse through the glass into the gel where they react, and reaction products diffuse back out into the flowing solutions where they are swept away and permanently removed. Thus the outer boundaries are also surfaces of zero concentration for the reaction products. The diameter of the plates (about 25 mm) are over 100 times larger than the typical length scale of the cellular patterns (about 0.2 mm) so that the system is approximately translationally invariant in the extended directions. In the actual experiment, no influence of the lateral boundaries was observed for the instability and resulting patterns, although a systematic study was not carried out by varying the diameter of the gel.

Evolution Equations

With this experiment in mind, we now discuss how to derive the evolution equations that mathematically describe the experiment. The small pores of the gel in Fig. 3 suppress any fluid motion so an evolution equation is not needed for the velocity, which is zero everywhere. It also turns out that the diffusion of heat is so fast compared to the diffusion of chemicals that the temperature field can be assumed to be constant and so does not evolve. The state of the system at any given time t is therefore given by the values at each point in space of continuously varying concentration fields $u_i(t, \mathbf{x})$, which have the meaning of the local concentration of the ith chemical at point $\mathbf{x}$ at time t. Note that the concentrations can be treated as continuous variables because the pattern formation occurs on a length scale of millimeters that is huge compared to the mean free path of collisions between molecules, of order nanometers.

The evolution equations for the system—together with mathematical descriptions of the boundaries and initial values for the concentration fields—determine how the concentration fields change from one moment in time to the next. The concentration fields change their values by two mechanisms. Chemical reactions change concentrations of reagents and of products according to the concentration values at each point in space. Diffusion by molecular collisions decreases the values of concentration fields where they are locally larger than surrounding values. We discuss these in turn and then combine their contributions to get the final evolution equations.

Let us first consider just the effects of chemical reactions by assuming that the chemical concentrations are spatially uniform so that diffusion can be ignored. (Diffusion can be eliminated experimentally by stirring the chemical solution at high speed.) Then the **rate of reaction** $\nu(t)$ for some chemical reaction is defined in terms of the time derivatives of concentrations and of stoichiometric coefficients [1]. For example, let us consider a binary chemical reaction in which a moles of molecules labeled A and b moles of molecules labeled B react to produce c moles of molecules labeled C and d moles of molecules labeled D. In standard notation, this reaction would be written in the form

$$a\,\mathrm{A} + b\,\mathrm{B} \rightarrow c\,\mathrm{C} + d\,\mathrm{D}. \tag{32}$$

The coefficients a, b, c, and d are the **stoichiometric coefficients** for molecules A, B, C, and D respectively. By definition, the reaction rate $\nu(t)$ for the entire reaction is the non-negative quantity given by

$$\nu(t) = -\frac{1}{a}\frac{d[\mathrm{A}]}{dt} = -\frac{1}{b}\frac{d[\mathrm{B}]}{dt} = \frac{1}{c}\frac{d[\mathrm{C}]}{dt} = \frac{1}{d}\frac{d[\mathrm{D}]}{dt}. \tag{33}$$

The notation $[X]$ denotes the concentration of molecule X.

For simple chemical reactions in gases or solutions, the reaction rate $\nu(t)$ is given by the **law of mass action**, which states that the reaction rate is proportional to the product of powers of reactant concentrations giving a **rate law**

$$\nu(t) = k[A]^{m_A}[B]^{m_B}, \tag{34}$$

with the powers $m_A = a$ and $m_B = b$ given by the stoichiometry factors. (Chemists call these powers the **orders** of the reaction with respect to the concentrations.) The positive proportionality constant k is called the **rate constant**. Reactions obeying this law are called **elementary reactions.** For reactions that are not elementary, the functional form Eq. (34) still sometimes applies but with exponents m_A and m_B whose values may be integers or half-integers that are not simply related to the stoichiometry and so need to be deduced from experiments. In the most general case, the reaction rate may be some arbitrary nonlinear function of the concentrations. Note that if the concentration of B is so large that it can be treated as constant, Eq. (34) takes the form

$$\nu(t) = -\frac{1}{a}\frac{d[\mathrm{A}]}{dt} = k_1[\mathrm{A}]^{m_A}. \tag{35}$$

The effective rate constant k_1 now depends on the concentration of B and so can be varied as a control parameter.

Let us next consider the effects of diffusion without chemical reaction. For each chemical species i, there is a chemical potential $\mu_i(t, \mathbf{x})$ that is the thermodynamic variable conjugate to the concentration field $u_i(t, \mathbf{x})$ of that species. Gradients in the chemical potentials drive currents of the chemicals, and, in turn, these currents can be related to gradients in the concentrations. To a good approximation, a gradient in the concentration of the ith species drives a current only of the ith concentration[8]. Thus we have a conservation equation

$$\partial_t u_i = -\nabla \cdot \mathbf{j}_i, \tag{36}$$

which states that the rate of change of the concentration u_i at a point $\mathbf{x}$ is given by the negative of the total flux of u_i into an infinitesimal region surrounding that point. In turn, the flux $\mathbf{j}_i$ of u_i at the point $\mathbf{x}$ is proportional to the gradient in the concentration of u_i[9]:

$$\mathbf{j}_i = -D_i \nabla u_i. \tag{37}$$

The positive number D_i is the **diffusion coefficient** for u_i and has SI units of m^2/s. These two equations can be combined to yield a diffusion equation

$$\partial_t u_i = \nabla \cdot (D_i \nabla u_i) = D_i \nabla^2 u_i, \tag{38}$$

where the last expression $D_i \nabla^2 u_i$ holds if the diffusion coefficient is constant, a good approximation for many experiments.

By combining the effects of reaction and diffusion, Eqs. (33), (34), and (38), we conclude that the evolution equations for the concentration fields $u_i(t, \mathbf{x})$ take the general reaction-diffusion form

$$\partial_t u_i = f_i(\{u_j\}) + D_i \nabla^2 u_i, \tag{39}$$

with one such equation for each chemical concentration. Here the ith chemical diffuses with a constant diffusion coefficient D_i and the reaction rates f_i are nonlinear functions of the chemical concentrations. For

[8] This statement is not as obvious as it might seem at first. For example, in Rayleigh-Bénard convection of a binary fluid mixture, a gradient in the temperature can drive a concentration current in addition to an energy current, a phenomenon known as the *Soret effect*.

[9] The direction of the concentration current $\mathbf{j}$ is the negative of the gradient since the gradient of a field ∇u points in the direction in which the field u increases most rapidly. A chemical flows in the opposite direction, from larger to smaller concentration values.

simple rate laws of the form Eq. (34), the f_i are multinomials in the concentrations u_i but more complicated nonlinear functions are common.

To obtain a unique solution to these evolution equations, further information is needed in the form of initial values of the concentration fields at some starting time t_0 and mathematical conditions describing how the boundaries constrain the fields. Since the reactor geometry of Fig. 3 has been constructed in such a way that the contents of the reservoirs flow quickly past the outer surfaces of plates A and B, to a good approximation each concentration field $u_i(t, \mathbf{x})$ corresponding to a reagent has a constant positive value on this outer surface equal to the concentration in the corresponding reservoir. The concentration of a reagent is zero on the opposing plate since the flowing solutions sweep away any of the chemical that reaches that side. For the same reason, the concentration fields corresponding to products are zero on the outer surfaces of both plates. Finally, the chemicals are sealed in by the lateral boundary of the gel and so all the concentration fields satisfy a zero-flux condition $\hat{n} \cdot \mathbf{j}_i = -D_i \hat{n} \cdot \nabla u_i = 0$ at each point on the lateral boundary, where $\hat{n}$ is the unit vector normal to the lateral boundary at a given point. These no-flux lateral conditions would typically be replaced by infinite or periodic boundary conditions when carrying out a linear stability analysis.

The derivation of equations such as Eq. (39) involves various approximations that are less well justified than those used to derive the evolution equations for fluids. With a few exceptions, a simple rate law of the form Eq. (34) holds only for elementary reactions in dilute solutions or for ideal gases. Whether some particular reaction is elementary can be difficult to establish experimentally. Further, the identification of the reaction mechanism—the sequence of elementary steps that lead from reagents through intermediates to final products—often requires separating the important reactions (those that are slower and so rate limiting) from a much larger list of possible reactions that produce various short-lived and often unknown intermediate molecules. This separation is a rather *ad hoc* procedure since there is no small parameter that can be exploited in a perturbation theory to improve the validity systematically.

In contrast, the fundamental approximation leading to the evolution equations for a fluid (the Navier-Stokes equation) is that the flow varies spatially over much larger distances than the microscopic scale set by the mean free path for molecular collisions. This is a *very* good approximation for typical laboratory fluid experiments whose spatial variations are millimeters or larger, and can be improved—if necessary—by increasing the size of the experiment.

Evolution Equations for the Chlorine Dioxide-Iodine-Malonic Acid (CDIMA) Reaction

Following recent work by the chemists I. Lengyel, G. Rábai, and I. Epstein [2, 3], let us write down the evolution equations for the pattern-forming Chlorine Dioxide-Iodine-Malonic Acid reaction (abbreviated CDIMA)that has been studied experimentally. In Fig. 3, reservoir A would contain chlorine dioxide ClO_2 and iodine I_2 which do not react together while reservoir B would contain malonic acid $CH_2(COOH)_2$ (abbreviated as MA). The reaction between the ClO_2, I_2, and MA molecules produces further reactants—the iodide I^- and chlorite ClO_2^- ions—as well as products that take no further part in the reaction. The iodide concentration $[I^-]$ is visualized with an immobile starch indicator S that is embedded in the gel and that turns blue reversibly upon binding to iodide.

By comparing theory and experiment for stirred CDIMA reactions such that diffusion did not play a role, the chemists proposed a simplified reaction mechanism consisting of the following four reactions:

$$\mathrm{MA} + \mathrm{I_2} \rightarrow \mathrm{IMA} + \mathrm{I^-} + \mathrm{H^+}, \tag{40a}$$

$$\mathrm{ClO_2} + \mathrm{I^-} \rightarrow \mathrm{ClO_2^-} + \frac{1}{2}\,\mathrm{I_2}, \tag{40b}$$

$$\mathrm{ClO_2^-} + 4\mathrm{I^-} + 4\mathrm{H^+} \rightarrow \mathrm{Cl^-} + 2\mathrm{I_2} + 2\mathrm{H_2}0, \tag{40c}$$

$$\mathrm{S} + \mathrm{I_2} + \mathrm{I^-} \rightleftharpoons \mathrm{SI_3^-}. \tag{40d}$$

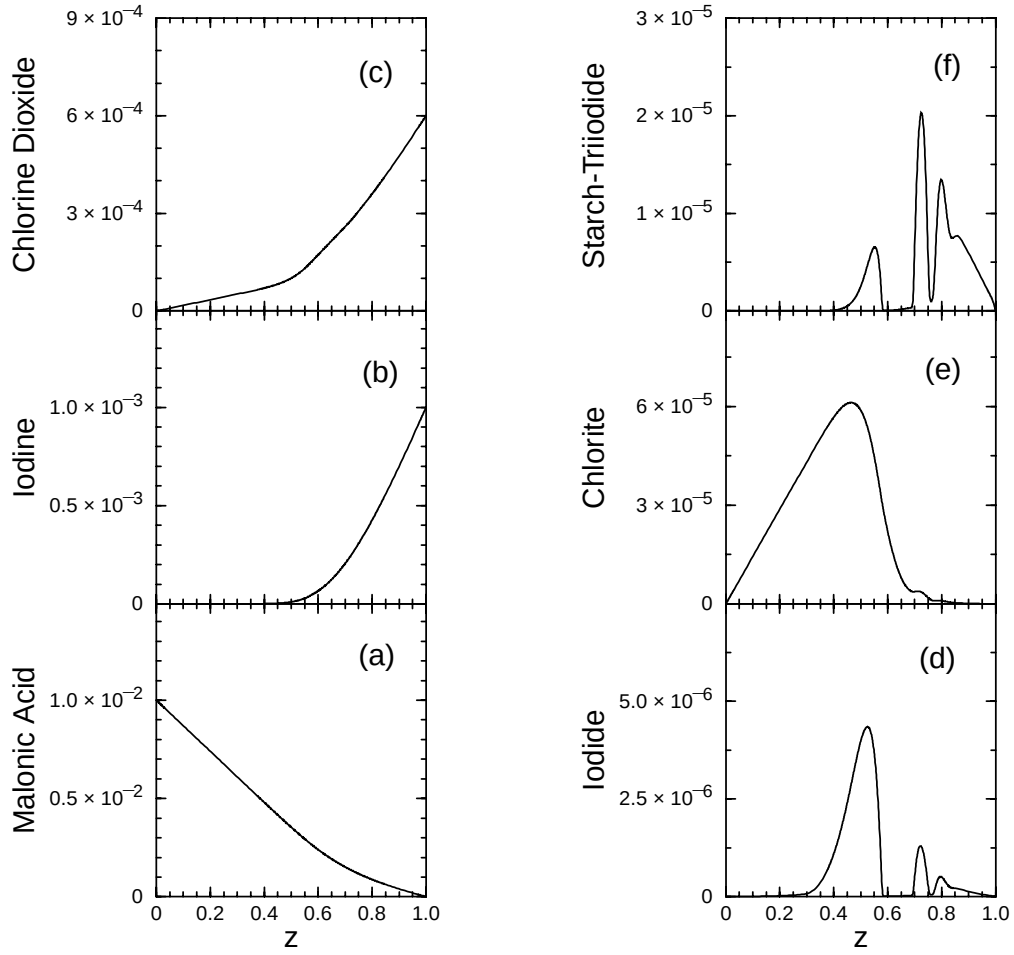

Figure 4: Numerically calculated profiles (chemical concentrations as a function of the confined coordinate $x_{\|} = z$) for the stationary uniform state of the CDIMA reaction, Eq. (40), in the reactor geometry of Fig. 3. The gel was assumed to have a thickness of $d = 0.3\,\mathrm{cm}$ and the z coordinate measures the fractional distance across the gel, with $z = 0$ corresponding to plate B and $z = 1$ corresponding to plate A. The boundary conditions are $[\mathrm{MA}]_L = 1 \times 10^{-2}$ M at the left boundary $z = 0$, and $[\mathrm{I_2}]_R = 1 \times 10^{-3}$ M and $[\mathrm{ClO_2}]_R = 6 \times 10^{-4}$ M at the right boundary $z = 1$. All other boundary conditions are zero concentration. Especially for the intermediates like iodide and the starch-triiodide complex, the profiles have a surprisingly complicated rapidly varying spatial structure. The concentrations are spatially uniform in each plane of constant z. [From the paper "Turing instability in a boundary-fed system," by S. Setayeshgar and M. C. Cross, Phys. Rev. E **59**, 4258 (1999)]

Since the reactions are sustained out of nonequilibrium, with new reagents ClO_2, I_2, and MA constantly being supplied and reaction products steadily being removed, we can assume that the reverse reactions for the first three equations proceed at a negligible rate. The reversible formation of the starch complex SI_3^- in Eq. (40d) plays a doubly important role in the pattern formation. First, this is the colored indicator that actually allows the pattern to be seen. Second, because this complex is fixed to the gel, the effective diffusion constants of the iodine and iodide are reduced since these molecules become immobile for the fraction of the time that they are bound to the starch. As we suggested in §, significantly different diffusion coefficients of at least two reactants are a necessary condition for the linear instability of a uniform state. This condition would be hard to attain without the immobile starch since the diffusion coefficients of small ions in solution are all comparable.

The comparisons of theory with experiment for the stirred CDIMA reaction suggest the following respective reaction rates $r_j(t)$:

$$r_1 = \frac{k_{1a}[\mathrm{MA}][\mathrm{I_2}]}{k_{1b} + [\mathrm{I_2}]}, \tag{41a}$$

$$r_2 = k_2[\mathrm{ClO_2}][\mathrm{I^-}], \tag{41b}$$

$$r_3 = k_{3a}[\mathrm{ClO_2^-}][\mathrm{I^-}][\mathrm{H^+}] + \frac{k_{3b}[\mathrm{ClO_2^-}][\mathrm{I_2}][\mathrm{MA}]}{h + [\mathrm{I^-}]^2}, \tag{41c}$$

$$r_4 = k_{4+}[\mathrm{S}][\mathrm{I^-}][\mathrm{I_2}] - k_{4-}[\mathrm{SI_3^-}]. \tag{41d}$$

The various parameters are determined by fits to experimental data. The reaction rates r_2 in Eq. (41b) and r_4 in Eq. (41d) have the simple form expected of an elementary reaction but the other two have more complicated nonlinear dependencies on the concentrations. This complexity can be partly understood as arising from the elimination of short-lived intermediate products from the rate equations. You should keep in mind that these reaction rates are plausible deductions from empirical data rather than obtained from first principles by a theoretical argument. It is even possible that the functional form of these expressions could change in the future since research still continues on how best to quantify the CDIMA system.

Using the definition of reaction rate Eq. (33) and allowing the chemicals to diffuse, we obtain the following six coupled evolution equations for the CDIMA pattern-forming system:

$$\partial_t[\mathrm{ClO_2}] = -r_2 + D_{\mathrm{ClO_2}}\nabla^2[\mathrm{ClO_2}], \tag{42a}$$

$$\partial_t[\mathrm{ClO_2^-}] = r_2 - r_3 + D_{\mathrm{ClO_2^-}}\nabla^2[\mathrm{ClO_2^-}], \tag{42b}$$

$$\partial_t[\mathrm{MA}] = -r_1 + D_{\mathrm{MA}}\nabla^2[\mathrm{MA}], \tag{42c}$$

$$\partial_t[\mathrm{I_2}] = -r_1 + \frac{1}{2}r_2 + 2r_3 - r_4 + D_{\mathrm{I_2}}\nabla^2[\mathrm{I_2}], \tag{42d}$$

$$\partial_t[\mathrm{I^-}] = r_1 - r_2 - 4r_3 - r_4 + D_{\mathrm{I^-}}\nabla^2[\mathrm{I^-}], \tag{42e}$$

$$\partial_t[\mathrm{SI_3^-}] = r_4. \tag{42f}$$

The linear combination of reaction rates in each equation follows from the corresponding stoichiometry in the reaction mechanism Eq. (40). There is no diffusion term in Eq. (42f) for the starch-triiodide complex since the starch is immobile. The values of the five diffusion coefficients have to be determined by experiment. Together with the parameters in the reaction rates Eq. (41), this system is described by a total of 13 parameters (which can be reduced to five dimensionless parameters by changing to dimensionless units of space, time, and concentration). In contrast, two dimensionless parameters—the Rayleigh number R and Prandtl number σ—are needed to characterize a Rayleigh-Bénard convection experiment. Each of the equations in Eq. (42) also requires boundary conditions and initial data to complete the mathematical description. As noted before, the boundary conditions have a simple form, being constant on the plate surfaces or having a zero flux on the lateral boundaries of the gel.

If no reactions were to occur within the gel, we would expect the concentrations [ClO_2], [MA], and [I_2] to interpolate linearly between their boundary values on either side of the plates. Such linear profiles would be analogous to the linear temperature profile of the conducting uniform state in Rayleigh-Bénard convection. In fact, the reactions in the interior of the gel produce a much more complicated set of profiles for the chemicals, with a z dependence that cannot be calculated analytically. A numerical calculation based on the above evolution equations with experimentally estimated parameters and with experimentally plausible concentrations in reservoirs A and B produce the concentration profiles of Fig. 4 [7]. The stationary concentrations are plotted as a function of a dimensionless confined variable $x_\parallel = z$, whose value is $z = 0$ at the surface of plate B and $z = 1$ at the surface of plate A. The six concentration fields are constant and uniform in each plane transverse to the z direction. This complicated structure—a direct consequence of the tight coupling to the strong chemical gradients imposed by the reservoirs—constitutes the "spatially uniform solution" that would be the starting point of a full linear stability analysis [8]. Pattern formation would then be the occurrence of spatial structure in the concentration fields within each plane transverse to z.

Besides the explicit example Eq. (42) of realistic evolution equations, perhaps the most important conclusion of this Étude is that the stationary uniform solution of a sustained nonequilibrium system can have a surprisingly rich structure in the confined directions even before pattern formation occurs in the extended directions. This structure can be quite hard to calculate—by no means can we always do this analytically.

Experimental Results

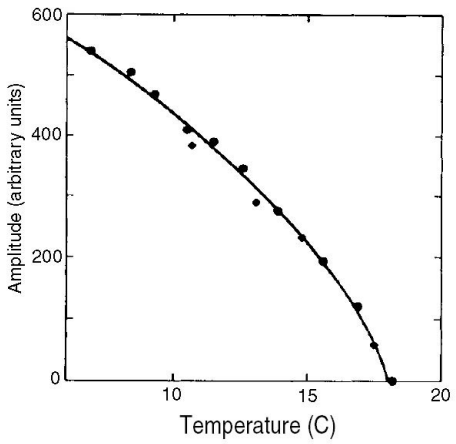

Figure 5: Patterns", by Q. Ouyang and H. L. Swinney, Nature **352**, 610 (1991)]

The quantitative analysis of the onset of the pattern is shown in Fig. 5. The order parameter used is the magnitude of the two dimensional Fourier transform integrated over a wave number band near the peak intensity. This is zero in the ideal spatially uniform state (noise in the experiment or measurement would contribute a small value), and is a good measure of the "amplitude of the pattern". The control parameter used in the experiment was the temperature: varying the temperature changes the rate constants for the various reactions. Typically different rate constants will vary by different amounts that must be measured experimentally if a quantitative link between this control parameter and the parameters of the theoretical model is desired. This has not yet been done. Figure 5 suggests a linear onset at around 18C.

For other chemical combinations wave states can observed as sustained states in a continuously fed reactor.

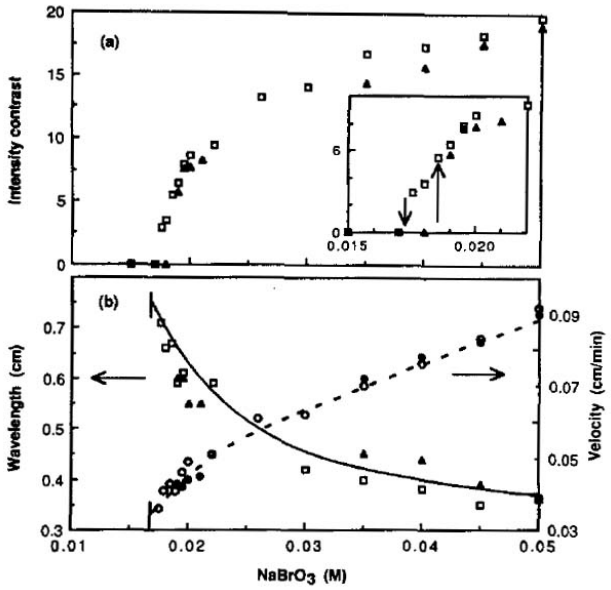

Figure 6: Reactor", by W. Y. Tam, W. Horsthemke, Z. Noszticzius, and H. L. Swinney, J. Chem. Phys. **88**, 3395 (1998)]

The more controlled conditions allow quantitative measurements to be made, as shown in Fig. 6. In this experiment the intensity contrast of the optical technique measuring the difference in indicator concentration between the wave crests and troughs was used as the order parameter. The measurements suggest a linear onset at about 0.018M sodium bromate concentration, although there is a small amount of hysteresis at the onset (so that the bifurcation is slightly subcritical, rather than supercritical) which makes a precise determination harder. Note that the wavelength and velocity of the waves (and therefore the frequency as well) tend to nonzero values at the onset, showing this to be a type I-o instability.

References

[1] Irving R. Epstein and John A. Pojman. *An Introduction to Chemical Dynamics: Oscillations, Waves, Patterns, and Chaos*. Oxford U. Press, New York, 1998.

[2] I. Lengyel, G. Rábai, and I. Epstein. Batch oscillation in the reaction of chlorine dioxide with iodine and malonic acid. *J. Am. Chem. Soc.*, 112:4606–4607, 1990.

[3] I. Lengyel, G. Rábai, and I. Epstein. Experimental and modeling study of oscillations in the chlorine dioxide-iodine-malonic acid reaction. *J. Am. Chem. Soc.*, 112:9104–9110, 1990.

[4] J. D. Murray. *Mathematical Biology*. Springer, Berling, Second edition, 1993.

[5] Q. Ouyang and Harry L. Swinney. Transition to chemical turbulence. *Chaos*, 1(4):411–420, 1991.

[6] Lee A. Segel and Julius L. Jackson. Dissipative structure: An explanation and an ecological example. *J. Theor. Bio.*, 37:545–559, 1972.

[7] S. Setayeshgar and M. C. Cross. Turing instability in a boundary-fed system. *Phys. Rev. E*, 58(4):4485–4500, 1998.

[8] S. Setayeshgar and M. C. Cross. Numerical bifurcation diagram for the two-dimensional boundary-fed chlorine-dioxide-iodine-malonic-acid system. *Phys. Rev. E*, 59(4):4258–4264, 1999.

[9] Alan Turing. The chemical basis of morphogenesis. *Phil. Trans. R. Soc. London*, 237:37–72, 1952.